

HIGH-CYCLE FATIGUE BEHAVIOR  
OF  
TYPE 316 STAINLESS STEEL AT  $593^{\circ}\text{C}$

MASTER

by

D. T. Raske

**DISCLAIMER**

Prepared for  
USDOE/UKAEA Exchange Meeting  
on  
Mechanical Properties for FBR Structural Materials  
Warrington, England  
September 22-24, 1980



DISTRIBUTION OF THIS DOCUMENT IS UNLIMITED

## ARGONNE NATIONAL LABORATORY, ARGONNE, ILLINOIS

**Operated under Contract W-31-109-Eng-38 for the  
U. S. DEPARTMENT OF ENERGY**

High-cycle Fatigue Behavior of Type 316 Stainless Steel  
at 593°C

D. T. Raske

Materials Science Division  
ARGONNE NATIONAL LABORATORY

Introduction

This report describes the initial results of a program to determine the high-cycle fatigue behavior of Type 316 stainless steel. The objective of this study is to provide in-air strain-life curves to  $10^8$  cycles at 482 and 593°C. These curves will be used to evaluate fatigue damage due to thermal striping in the upper core components of CRBR.<sup>1</sup> This program is being conducted in collaboration with EG&G Idaho, Inc., and will consist of studies on the effects of cyclic frequency, surface finish, periodic overloads, heat-to-heat variability, thermal aging, mean stresses, and irradiation in addition to the base-line study.

Scope

The present report contains the current high-cycle fatigue results at 593°C and a preliminary strain-life curve fit to all the available data between 593 and 600°C.

Experimental Program

Materials and Specimens. Type 316 stainless steel plate from the reference heat 8092297 was used in this investigation. Axially loaded uniform-gauge specimens were machined longitudinally to the plate-rolling direction and solution annealed at 1065°C for 30 min prior to testing. The average grain size was 56  $\mu\text{m}$  (ASTM 5). A gauge-section surface finish of 0.2  $\mu\text{m}$  (8  $\mu\text{in.}$ ) was obtained by mechanical polishing prior to the heat treatment. The pertinent specimen dimensions are shown in Fig. 1. Originally, the specimen gauge section had a 0.001-in. (0.03-mm) taper which resulted in a uniform strain distribution

over the section.<sup>2</sup> In the present study, however, concern over failures outside the extensometer gauge section led to the adoption of a 0.002 to 0.0025-in. (0.05-0.06 mm) taper which resulted in a slightly higher (~1%) strain in the critical section.

Apparatus and Test Procedure. The tests were conducted on closed-loop hydraulic test machines at 593°C in air with cyclic frequencies up to ~20 Hz. The control mode was axial stroke and the cyclic strain ranges were maintained by periodically reducing the test frequency and monitoring the signal from an axial extensometer. The test setup is shown schematically in Fig. 2 and described in detail in Ref. 3. As shown, the specimen was heated by an induction coil operating at 455 kHz. The coil was designed to provide a relatively flat temperature profile ( $\pm 3^\circ\text{C}$ ) over the critical gauge section.

A typical history of the test frequencies employed with the stroke/strain control method is shown in Fig. 3. Initially, the frequency is kept low during the rapid cyclic hardening period so that the correct strain range can be carefully monitored and maintained. This includes the first overnight period, when unattended high-frequency cycling could result in strain ratchetting and a subsequent mean strain. After this initial period, the frequency is only periodically reduced for minor stroke adjustments to maintain the correct strain range.

#### Results

The results of tests completed and in progress are listed in Table 1. All but one of the ANL tests listed were conducted using the stroke/strain method of control described previously. The exception is a test (no. 284) which is a replicate of a test conducted by EG&G Idaho.<sup>4</sup> This test was started in

strain control at a strain rate of  $4 \times 10^{-3} \text{ s}^{-1}$ . At  $1.2 \times 10^6$  cycles the control mode was changed to load and the strain rate to  $1.2 \times 10^{-1} \text{ s}^{-1}$  (20 Hz). The results will be used for strain-rate effects and interlaboratory variability data. Of the seven tests completed at ANL, three failures were initiated at a subsurface inclusion. An energy-dispersive x-ray analysis of a typical inclusion indicated that it was rich in silicon, molybdenum, and copper. The failures that were not initiated in this manner had a large area ( $\sim 2 \text{ mm}^2$ ) beneath the surface which appeared to be a metallurgical notch. Further study in this area is currently underway.

Typical cyclic hardening behavior observed in these tests is shown in Fig. 4. In most of the low strain-range tests ( $\Delta\epsilon \leq 0.30\%$ ) at ANL, the hysteresis loop trace and load values would indicate fully elastic conditions at around  $\sim 7 \times 10^5$  cycles. For the other tests, small inelastic strains would persist throughout the life of the specimen.

The data from Table 1 were combined with the available low- and high-cycle fatigue data at  $593-600^\circ\text{C}$ <sup>4-6</sup> to provide a preliminary strain-life curve. This curve, shown in Fig. 5, is based on 74 test data including 2 run-outs (suspended tests) and, for the present, is considered to be independent of strain-rate, heat-to-heat, and heat-treatment effects. In order to determine this curve, the data were fit to a nonlinear relation of the form

$$\log(\log N_f) = \beta_0 \log(\Delta\epsilon + \beta_1) + \beta_2, \quad (1)$$

where  $N_f$  is the fatigue life and  $\Delta\epsilon$  the strain range in percent. The log-log transformation on  $N_f$  was employed because the results of a study on the variability of fatigue data indicate that this is the appropriate transformation of the logarithmic type. Thus, the log-log transformation results in a more nearly

uniform and normal distribution of the residual error terms than does the usual log transformation. This means that the least-squares estimators,  $\beta_1$ , will have a minimum variance<sup>7</sup> and consequently more confidence can be placed in the location of this curve in the critical high-cycle regime. The two run-out data were treated by an iterative least-squares procedure where successive estimates of the probable fatigue life are made until convergence is obtained.<sup>8</sup> After this analysis, the relation given in Eq. (1) can be inverted analytically to give the more convenient form

$$\Delta\epsilon = 55.90(\log N_f)^{-3.502} + 0.214 . \quad (2)$$

Based on this correlation, the current estimate of strain range for a life of  $10^8$  cycles is 0.25%.

Modifying Eq. (2) by the appropriate safety factors to obtain a design curve analogous to those in ASME Code Case N-47<sup>9</sup> gives the curve shown in Fig. 6. As indicated, the curves diverge beyond  $\sim 10^4$  cycles. Indeed, the new curve shown increases the allowable number of cycles by more than two orders of magnitude compared with the ASME curve at a strain range of  $\sim 0.14\%$  ( $\sim 10^7$  vs  $\sim 10^5$  cycles).

As the high-cycle data base evolved, the existence of significant strain-rate effects became apparent. This is illustrated in Fig. 7 which is an expanded plot of the high-cycle data. The curve shown in this figure is the regression analysis curve from Fig. 5. Note that the tests conducted with a 1Hz sine wave have the shortest fatigue lives. This is attributed to the low actual strain rate at the peak strain compared to the constant strain rates in the other tests. Current efforts at ANL include a study of this effect.

Summary

The available low- and high-cycle fatigue data on Type 316 stainless steel at 593-600°C have been combined and analyzed to provide a preliminary strain-life correlation. This correlation was then reduced by the appropriate safety factors to a design curve and compared with the ASME T-1420-1B curve. The comparison indicates that significant increases in allowable fatigue cycles should be realized when the present study is concluded.

## References

1. C. R. Brinkman, "Results of Program Planning Meeting on High Cycle Fatigue Behavior of Type 316 Stainless Steel," letter to Distribution, November 14, 1979.
2. D. T. Raske, "Low-Cycle Fatigue and Cyclic Deformation Behavior of Type 16-8-2 Weld Metal at Elevated Temperature," pp. 57-72 in *Fatigue Testing of Weldments, ASTM STP 648*, D. W. Hoeppner, Ed., American Society for Testing and Materials, 1978.
3. S. Majumdar, D. T. Raske, and W. F. Burke, "A Procedure for Strain-Controlled High-Cycle Fatigue Testing at Elevated Temperatures," to be published in *J. Test. Eval.* (Jan. 1981 issue).
4. Personal communication, G. E. Korth, EG&G Idaho, Inc., to D. T. Raske, Argonne National Laboratory, 1980.
5. D. R. Diercks, *A Compilation of United States and British Elevated-Temperature, Strain-Controlled Fatigue Data on Type 316 Stainless Steel*, Argonne National Laboratory, ANL/MSD-78/4, March 1978.
6. Personal communication, C. E. Jaske, Battelle Columbus Laboratories, to D. T. Raske, Argonne National Laboratory, June 1979.
7. J. Neter and W. Wasserman, *Applied Linear Statistical Models*, Richard D. Irwin, Inc., 1974.
8. J. Schmee and G. J. Hahn, "A Simple Method for Regression Analysis with Censored Data," *Technometrics* 21(4):417-432 (1979).
9. American Society of Mechanical Engineers, *ASME Boiler and Pressure Vessel Code, Case N47-15*, 1979.

Table 1. Results of High-cycle Fatigue Tests on Type 316 Stainless Steel<sup>a</sup> at 593°C

Laboratory	Test Number	Specimen Number	Strain Range, % <sup>b</sup>		Stress Range, MPa	Strain Rate, s <sup>-1</sup>	Fatigue Life	
			$\Delta\epsilon_t$	$\Delta\epsilon_p$			$N_f$	$t_f, h$
ANL	258 <sup>c</sup>	GR4-1	0.35	0.08	444	$4 \times 10^{-3}$ <sup>d</sup>	$9.18 \times 10^4$	45
	268	PU12	0.33	0.036	438	$5.6 \times 10^{-3}$ <sup>d</sup>	$7.87 \times 10^5$	257
	272	PU13	0.33	0.027	454	$1.56 \times 10^{-2}$ <sup>d</sup>	$1.219 \times 10^6$	144
	275	PU1	0.30	0.00	449	$1.10 \times 10^{-1}$ <sup>d</sup>	$29.99 \times 10^6$	455
	280	PU3	0.30	0.011	432	$1.12 \times 10^{-1}$ <sup>d</sup>	$31.23 \times 10^6$	464
	284	PU8	0.30	0.017	423	$4 \times 10^{-3}$	$6.61 \times 10^6$	577
	278	PU4	0.28	0.00	419	$1.07 \times 10^{-1}$ <sup>d</sup>	$165.78 \times 10^6$	2417
	286 <sup>e</sup>	PU5	0.28	0.00	419	$3 \times 10^{-2}$ <sup>f</sup>		
	287 <sup>e</sup>	PU9	0.30					
INEL	DR-6	0.35	0.043		480	$4 \times 10^{-3}$	$2.43 \times 10^5$	118
	DR-3	0.35	0.085		404	$4 \times 10^{-3}$	$5.46 \times 10^5$	266
	DR-9	0.32	0.023		449	$4 \times 10^{-3}$	$9.11 \times 10^5$	405
	DR-17	0.30	0.019		440	$4 \times 10^{-3}$	$3.42 \times 10^6$	521
	DR-27	0.29	0.026		426	.. <sup>g</sup>	$1.68 \times 10^6$	343
	DR-22	0.28	0.013		411	.. <sup>g</sup>	$8.75 \times 10^6$	393
	DR-23	0.27	0.010		399	.. <sup>g</sup>	$1.30 \times 10^6$	245
	DR-8	0.27	0.013		385	.. <sup>g</sup>	$3.65 \times 10^6$	367
	DR-24	0.26	0.014		381	.. <sup>g</sup>	$10.78 \times 10^6$	373
		0.25 <sup>e</sup>						
W-ARD		~0.29	..	..		$\sim 6 \times 10^{-3}$	$1.1 \times 10^7$	~450

<sup>a</sup>Heat 8092297 solution annealed at 1065°C for 30 min after final polishing.

<sup>b</sup> $\Delta\epsilon_t$  = total strain range,  $\Delta\epsilon_p$  = plastic strain range at  $N_f/2$ .

<sup>c</sup>Heat 65808.

<sup>d</sup>Average over entire life.

<sup>e</sup>Test in progress.

<sup>f</sup>Strain-rate effects test.

<sup>g</sup>1Hz Sine-wave loading pattern.

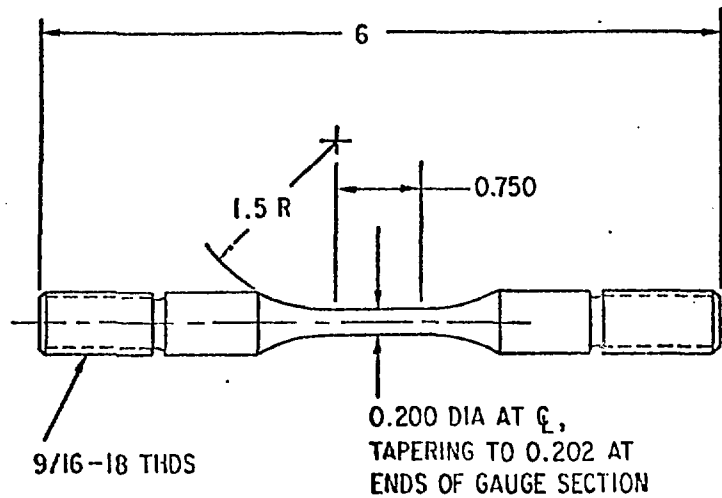


Fig. 1. ANL High-cycle Fatigue Specimen.

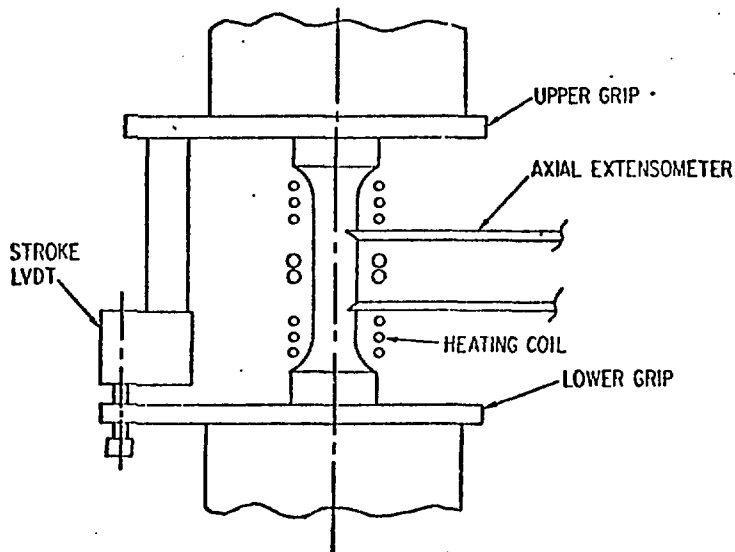


Fig. 2. Schematic Illustration of the High-cycle Fatigue Test Setup.

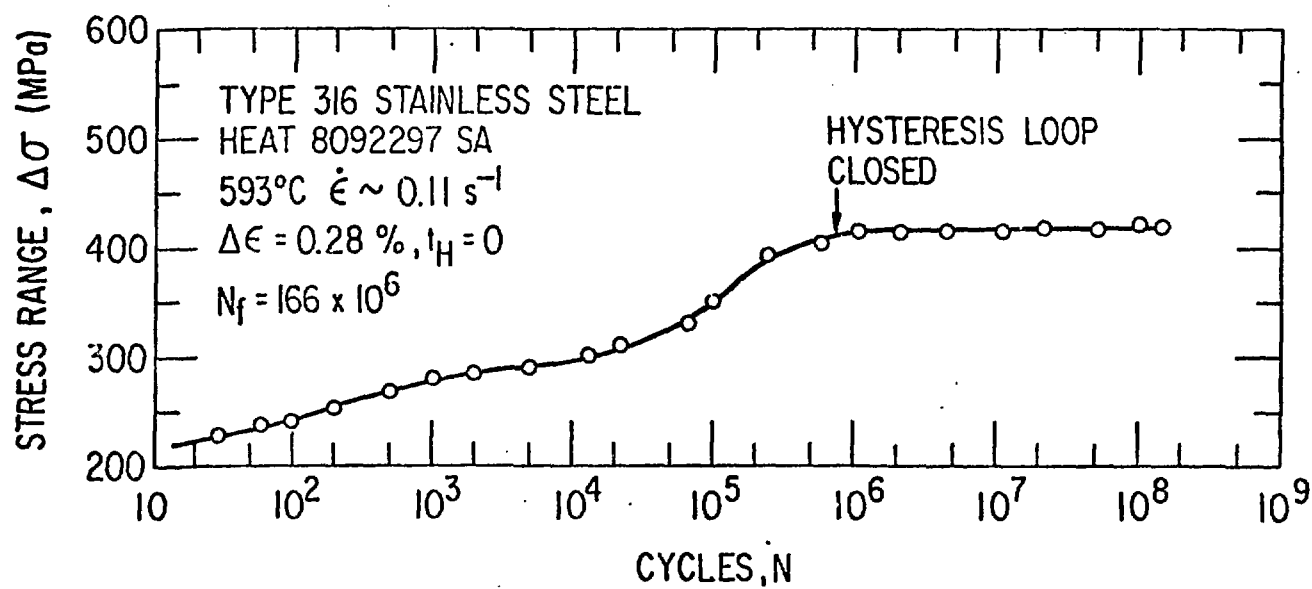
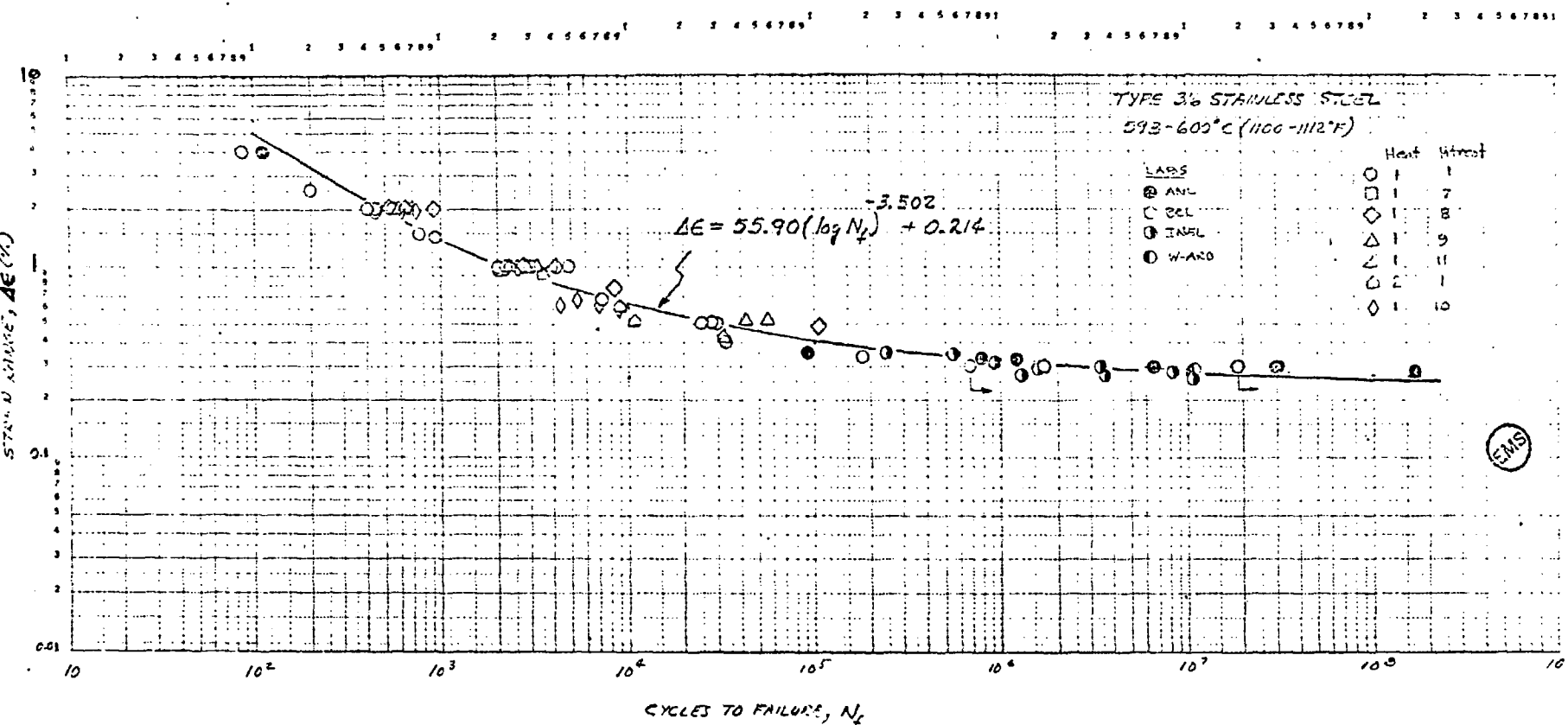


Fig. 4. Typical Cyclic Hardening Behavior for Low Strain-range Tests.



KoE SEMI-LOGARITHMIC 7 Cycles X 60 DIVISIONS  
KELFEL & ISSEI CO. MADE IN USA

46 6460

7-1-80  
8-21-80

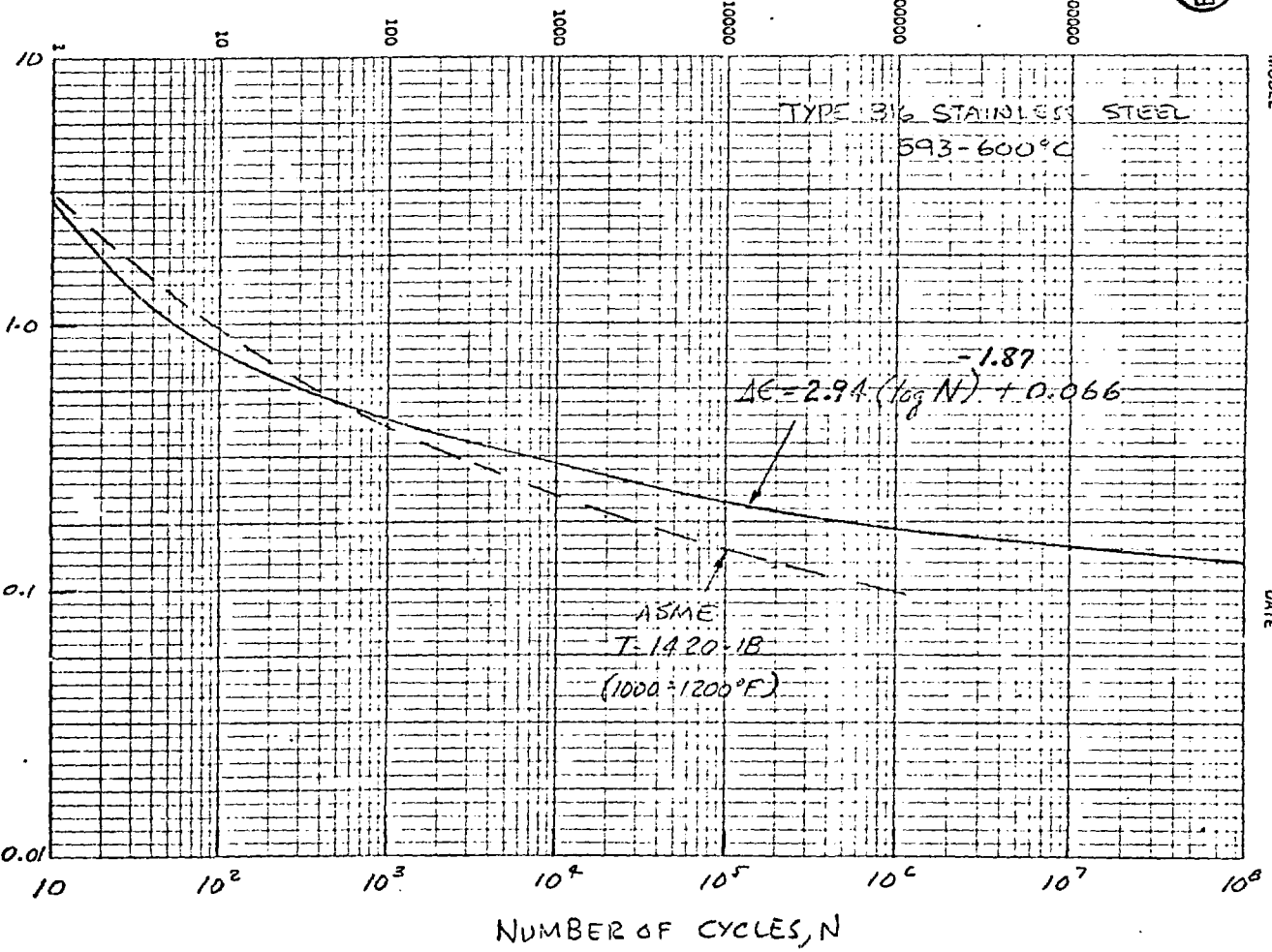


Fig. 6. Comparison of Design Curves.

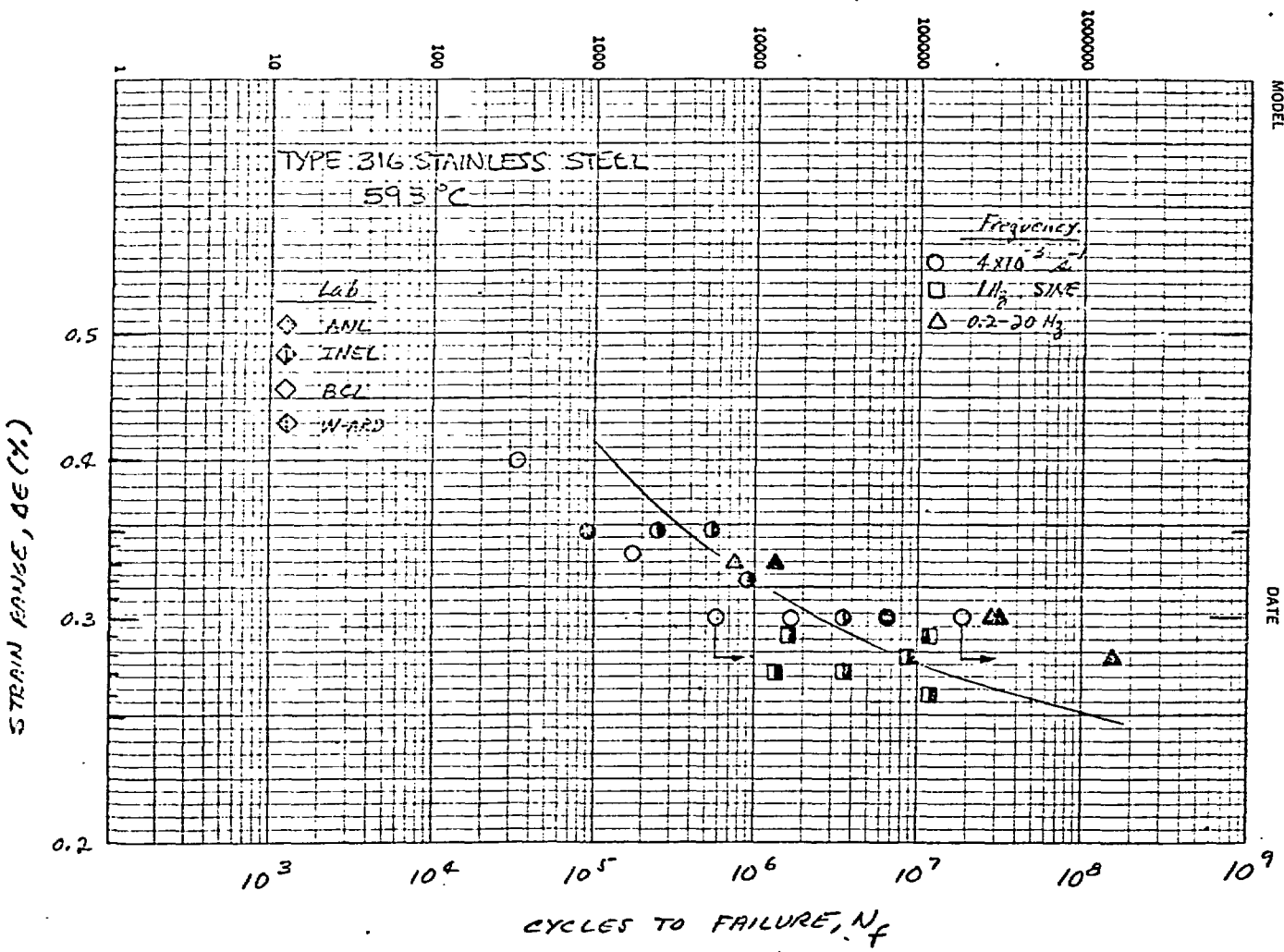


Fig. 7. High-cycle Fatigue Data.